CD151 Regulates Tumorigenesis by Modulating the Communication between Tumor Cells and Endothelium

Rafal Sadej,[1] Hanna Romanska,[2] Gouri Baldwin,[1] Katerina Gkirtzimanaki,[5] Vera Novitskaya,[1] Andrew D. Filer,[3] Zuzana Krcova,[6] Renata Kusinska,[4] Jiri Ehrmann,[6] Christopher D. Buckley,[3] Radzisław Kordek,[4] Piotr Potemski,[4] Aristides G. Eliopoulos,[5] El-Nasir Lalani,[7] and Fedor Berditchevski[1]

[1]Cancer Research UK Institute for Cancer Studies, [2]Department of Pathology and [3]Division of Immunity and Infection, The University of Birmingham, Edgbaston, Birmingham, United Kingdom; [4]Department of Pathology and Chemotherapy, Medical University of Łódź, Łódź, Poland; [5]Division of Basic Sciences, Laboratory of Molecular and Cellular Biology, University of Crete Medical School, Heraklion, Crete, Greece; [6]Department of Pathology, Laboratory of Molecular Pathology, Faculty of Medicine and Dentistry, Palacky University Olomouc, Olomouc, Czech Republic; and [7]Department of Pathology and Microbiology, Aga Khan University, Karachi, Pakistan

Abstract

The tetraspanin CD151 forms stoichiometric complexes with laminin-binding integrins (e.g., α3β1, α6β1, and α6β4) and regulates their ligand-binding and signaling functions. We have found that high expression of CD151 in breast cancers is associated with decreased overall survival (3.44-fold higher risk of death). Five-year estimated survival rates were 45.8% (95% confidence interval, 16.4-71.4%) for CD151-positive patients and 79.9% (95% confidence interval, 62.2-90.0%) for CD151-negative patients. Furthermore, CD151 was positively associated with axillary lymph node involvement. To study the biological significance of this observation, we investigated the contribution of CD151 in breast cancer tumorigenesis using MDA-MB-231 cells as a model system. Stable down-regulation of this tetraspanin by short-hairpin RNA decreased the tumorigenicity of these cells in mice. Detailed immunohistologic analysis of CD151 (+) and CD151(–) xenografts showed differences in tumor vascular pattern. Vascularization observed at the subcutaneous border of the CD151(+) tumors was less pronounced or absent in the CD151(–) xenografts. *In vitro* experiments have established that depletion of CD151 did not affect the inherent proliferative capacity of breast cancer cells in three-dimensional extracellular matrices, but modified their responses to endothelial cells in coculture experiments. The modulatory activity of CD151 was dependent on its association with both α3β1 and α6β4 integrins. These data point to a new role of CD151 in tumorigenesis, whereby it functions as an important regulator of communication between tumor cells and endothelial cells. These results also identify CD151 as a potentially novel prognostic marker and target for therapy in breast cancer. (Mol Cancer Res 2009;7(6):787–98)

Received 12/20/08; revised 3/5/09; accepted 3/19/09; published OnlineFirst 6/16/09.
Grant support: Cancer Research UK grants C1322/A5705 (F. Berditchevski). Z. Krcova and J. Ehrmann were supported by the Czech Ministry of Education Grant MSM 6198959216.
The costs of publication of this article were defrayed in part by the payment of page charges. This article must therefore be hereby marked *advertisement* in accordance with 18 U.S.C. Section 1734 solely to indicate this fact.
Note: Supplementary data for this article are available at Molecular Cancer Research Online (http://mcr.aacrjournals.org/).
Requests for reprints: Fedor Berditchevski, Cancer Research UK Institute for Cancer Studies, The University of Birmingham, Edgbaston, Birmingham B15 2TT, United Kingdom. Phone: 44-121-414-2801; Fax: 44-121-414-4486. E-mail: f.berditchevski@bham.ac.uk

doi:10.1158/1541-7786.MCR-08-0574

Introduction

Transmembrane proteins of the tetraspanin superfamily are the main structural unit of tetraspanin-enriched microdomains that are implicated in various cellular functions including motility, differentiation, and cell-cell fusion (1-3). It has been proposed that the functionality of the tetraspanin-enriched microdomain relies on the associated transmembrane receptors (e.g., adhesion molecules and receptor tyrosine kinases), the ligand binding and subsequent activities of which are influenced by specific tetraspanins (2, 4).

Various tetraspanins are also linked to tumorigenesis as having both protumorigenic and antitumorigenic activities. Overexpression of CD9 and CD82/KAI1 suppressed proliferation, tumorigenicity, and metastatic progression of various types of tumor cells (5-9). These *in vitro* data have been supported by observations of decreased expression of CD9 and CD82 in patients with advanced disease. The involvement of these tetraspanins in signaling and trafficking of the associated receptors (e.g., integrins, EGFR) may, in part, explain their role in tumor cell growth and metastatic spread (10, 11). In contrast, CO-O29, the overexpression of which was observed in various epithelial tumors, potentiates tumor cell growth *in vivo* by inducing tumor angiogenesis (12). Proangiogenic function of CO-029–expressing cells was linked to tumor-derived exosomes which stimulated angiogenesis both *in vitro* and *in vivo*. These results indicate that tetraspanins can regulate various steps (both for and against) in the tumorigenic process.

The tetraspanin CD151/PETA-3/SFA-1/Tspan24 forms highly stable complexes with a number of integrins including α3β1. Elevated expression of CD151 has been observed in patients with advanced forms of non–small cell lung carcinomas and prostate cancers (13, 14). Furthermore, previous reports have shown that although CD151 did not influence tumor cell growth at the primary site, it potentiated the metastatic properties of

tumor cells (15, 16). These data are in agreement with numerous *in vitro* experiments which identified CD151 as a promigratory and proinvasive tetraspanin (16-22). It has been proposed that CD151 regulates tumor cell invasion through mechanisms involving associated integrins, receptor tyrosine kinase c-Met, and matrix metalloproteinase-7 (23). More recently, it was found that elevated expression of CD151 was observed in high-grade and estrogen receptor (ER)–negative subtypes of breast cancers (24). This was further correlated with the ability of CD151 to facilitate the collaboration of $\alpha 6$ integrins with epidermal growth factor (EGF) receptor (EGFR; ref. 24).

In this article, we confirmed that elevated expression of CD151 is observed in high-grade breast cancers. Furthermore, for the first time, we showed that expression of this tetraspanin was a significant negative prognostic indicator of overall survival in breast cancer. However, in contrast to a recent publication by Yang and colleagues (24), we found that there was no correlation between the expression levels of CD151 and ER. Using MDA-MB-231 breast cancer cells as a model system, we have shown the contribution of CD151 to tumorigenesis and found that CD151 regulates tumor cell responses to soluble factors secreted by endothelial cells.

Results

Elevated Expression of CD151 Correlates with Lower Survival of Patients with Breast Cancer

To examine the potential involvement of CD151 in breast cancer, we did immunohistochemical analyses on the archival specimens from invasive ductal carcinoma. The median follow-up period for 42 censored patients was 54 months (range, 9-63), and for the whole group, it was 48.5 months (range, 1-63). During follow-up, two deaths due to causes other than breast cancer were observed. Patient characteristics are summarized in Supplementary Table S1. Seventeen (30.4%) cases were identified immunohistochemically as being CD151-positive (Fig. 1A, *top*), whereas 39 tumors were regarded as being CD151-negative (Fig. 1A, *bottom*). Associations between clinicopathologic variables and overall survival are presented in Table 1. CD151-positive patients had 3.44-fold higher risk of death from breast cancer in comparison with CD151-negative patients. The 5-year estimated survival rate was 45.8% [95% confidence interval (CI), 16.4-71.4%] for CD151-positive patients and 79.9% (95% CI, 62.2-90.0%) for the CD151-negative group (log rank $P = 0.016$; Fig. 1B). Interestingly, additional analysis showed that CD151 expression was positively associated with the involvement of regional lymph nodes ($P = 0.036$). Importantly, in contrast to a recently published report, we found no association of CD151 expression with ER status ($P = 0.640$). In addition, no correlation with tumor grade ($P = 0.810$), disease stage ($P = 0.339$), or age ($P = 0.773$) was observed. However, in a group of 31 patients with metastases in regional lymph nodes, CD151 expression showed a clear tendency towards worsening of overall survival (hazard ratio of death, 2.89; 95% CI, 0.82-10.19; $P = 0.098$).

Down-Regulation of CD151 Diminishes the Tumorigenic Potential of Breast Cancer Cells

Histologic Analysis of CD151-Positive and CD151-Negative Xenografts. To assess the contribution of CD151 to the tumorigenic process, we did xenograft experiments using a pair MDA-MB-231–derived cell lines which express high and low levels of CD151 referred to as MDA-MB-231/CD151(+) and MDA-MB-231/CD151(−) cells. The expression level of CD151 in MDA-MB-231/CD151(−) cells was >90% lower when compared with that of MDA-MB-231/CD151(+) cells (25). The tumorigenicity of these cells was assessed following xenotransplantation in athymic nude mice. As shown in Fig. 2A, the growth of MDA-MB-231/CD151(−) cells was slower with mean tumor sizes being ~2-fold smaller by 21 days when compared with MDA-MB-231/CD151(+) cells. Detailed histologic analysis was carried out to compare patterns of tumor growth in animals injected with CD151-positive and CD151-negative MDA-MB-231 cells. Both CD151(+) and CD151(−) tumor

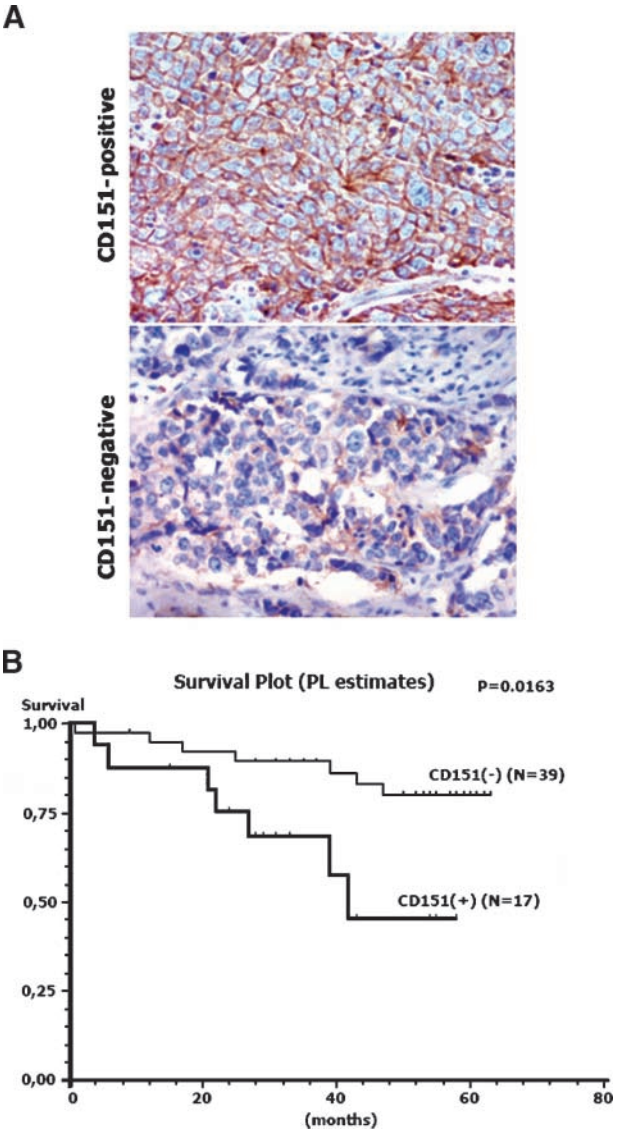

FIGURE 1. **A.** Positive (*top*) and negative (*bottom*) immunostaining for CD151 in breast cancer specimens (magnification, ×200). **B.** Kaplan-Meier estimate for overall survival in relation to CD151 expression. CD151 expression is associated with poorer prognosis. Five-year overall survival rate for CD151-positive patients was 79.9% as compared with 45.8% for CD151-negative patients (95% CI; hazard ratio, 3.44).

Table 1. Associations between Clinicopathologic Variables and Overall Survival

Variable	Hazard Ratio (95% CI)	*P*
Age (y)		
<50 vs ≥50	1.59 (0.55-4.61)	0.389
Disease stage		
III vs I-II	0.87 (0.27-2.77)	0.813
Grading		
3 vs 1-2	1.29 (0.43-3.85)	0.652
Nodal status		
Positive vs negative	3.53 (0.98-12.65)	0.053
ER status		
Positive vs negative	0.14 (0.03-0.62)	0.001
CD151 status		
Positive vs negative	3.44 (1.18-10.04)	0.024

nodules were composed of densely packed sheets of epithelioid cells with pleomorphic nuclei, many containing prominent nucleoli. In most CD151(+) tumors, there was central geographic necrosis, hemorrhage with an associated inflammatory infiltrate. At the subcutaneous margin of the CD151(+) xenografts, tumor nodules were clearly demarcated from the epidermis by bands of loose tissue composed of interwoven strands of fibrin, endothelial and mesenchymal cells, and infiltrated by granulocytes and lymphocytes (Fig. 2B and D). By contrast, CD151-negative xenografted tumor cells infiltrated the dermis with no apparent boundary between the tumor nodule and the epidermis (Fig. 2B). There was also less subcutaneous inflammation and intratumoral necrosis when compared with the CD151(+) tumors. Prevalence of necrotic areas in CD151(+) xenografts might have been due to the larger size of the tumors. The proliferative capacity of MDA-MB-231/CD151(+) and MDA-MB-231/CD151(−) cells *in vivo* was assessed by immunostaining of xenograft sections with antibody to Ki-67, a widely accepted marker of cell proliferation (26). The overall Ki-67 labeling index in CD151(−) xenografts was decreased when compared with CD151(+) tumors (90.00 ± 3.267 versus 108.7 ± 6.005, respectively; $P = 0.0145$; Fig. 2C). When specific regions of the tumors were analyzed, the results showed that differences in cell proliferation between CD151(+) and CD151(−) xenografts were most pronounced at the deep border of the tumors: 154.8 ± 5.69 for CD151-positive tumors versus 119.0 ± 5.080 for CD151-negative tumors ($P < 0.0001$).

To analyze the inflammatory response of the host and vascularization of the xenografts, consecutive sections were immunostained for F4/80, a marker of murine macrophages (27), and *Lycopersicon esculentum* lectin, which reacts with murine endothelium (28), respectively. In both MDA-MB-231/CD151(+) and MDA-MB-231/CD151(−) xenografts, F4/80-expressing cells were found scattered throughout the tumor with higher numbers at the margin of the tumors. This gradient was more pronounced in CD151(+) tumors (Fig. 3A). Although overall quantitative assessment of vessel density did not show significant difference between the two types of xenografts [CD151 (+), 5.37 ± 0.3150; CD151(−), 4.67 ± 0.199; $P = 0.2977$; 95% CI], vascularization of xenografts differed in the pattern of vessel distribution. Specifically, an angiogenic network at the subcutaneous border was better developed in CD151-positive tumors (Fig. 3A and B). MDA-MB-231 cells are known to secrete proangiogenic growth factors, vascular endothelial growth factor (VEGF) and basic fibroblast growth factor, which contribute to the growth and vascularization of xenografts *in vivo* (29, 30). However, we found that the control and MDA-MB-231/CD151(−) cells produced similar amounts of these proteins under standard culturing conditions, and there was no difference in either intensity or distribution of VEGF and basic fibroblast growth factor between the xenografts (Supplementary Fig. S1). Furthermore, we found that morphogenesis of cultured human umbilical vascular endothelial cells (HUVEC) on Matrigel was affected in equal measure by growth medium conditioned with MDA-MB-231/CD151(+) and MDA-MB-231/CD151(−) cells (Fig. 3C). These results suggest that different patterns of angiogenesis of MDA-MB-231/CD151(+) and MDA-MB-231/CD151(−) xenografts are likely to be a result of differences in cooperation between growing tumor cells and the host microenvironment.

The Role of CD151 in the Growth of Breast Cancer Cells in Three-dimensional Extracellular Matrix

As a first step towards understanding how CD151 can regulate tumor cell growth *in vivo*, we compared the behavior of MDA-MB-231/CD151(+) and MDA-MB-231/CD151(−) cells embedded in 0.16% collagen type I gels and Matrigel. Within 7 to 8 days after plating in collagen, both MDA-MB-231/CD151(+) and MDA-MB-231/CD151(−) cells formed extensive networks of cables/cords (Fig. 4A). Quantification of these experiments has shown that depletion of CD151 had no observable effect on length, thickness, or branching of the cables formed in three-dimensional collagen (results are not shown). When grown within three-dimensional Matrigel, both MDA-MB-231/CD151(+) and MDA-MB-231/CD151(−) cells formed compact colonies (Fig. 4B). Morphometric analysis of the colonies (i.e., colony diameter measurement) showed that a deficiency in CD151 does not change the inherent proliferative potential of MDA-MB-231 cells in three-dimensional extracellular matrix (ECM; Fig. 4C). This was subsequently confirmed when we measured the proliferation of MDA-MB-231/CD151 (+) and MDA-MB-231/CD151(−) cells in three-dimensional Matrigel using Alamar blue (Fig. 4D).

CD151 Regulates the Responses of Tumor Cells to Endothelial Cells but not Fibroblasts

We hypothesized that the inhibitory effect of CD151 depletion on growth *in vivo* may be due to the involvement of this tetraspanin in the communication between tumor cells and the surrounding stromal cells. First, we examined whether the presence of fibroblasts originated from various tissues affecting the growth of MDA-MB-231 cells in three-dimensional ECM. In these experiments, MDA-MB-231 cells were seeded in three-dimensional ECM over the monolayer of fibroblasts grown on plastic. We found that there was no migration of fibroblasts into three-dimensional ECM under these experimental conditions. When compared with the control conditions (i.e., culturing alone), coculturing with fibroblasts potentiated the growth of both CD151-positive and CD151-negative cells which developed more elaborate networks of cables in three-dimensional collagen within 7 to 8 days after plating (Fig. 5A). The pattern of growth and various morphometric variables (e.g.,

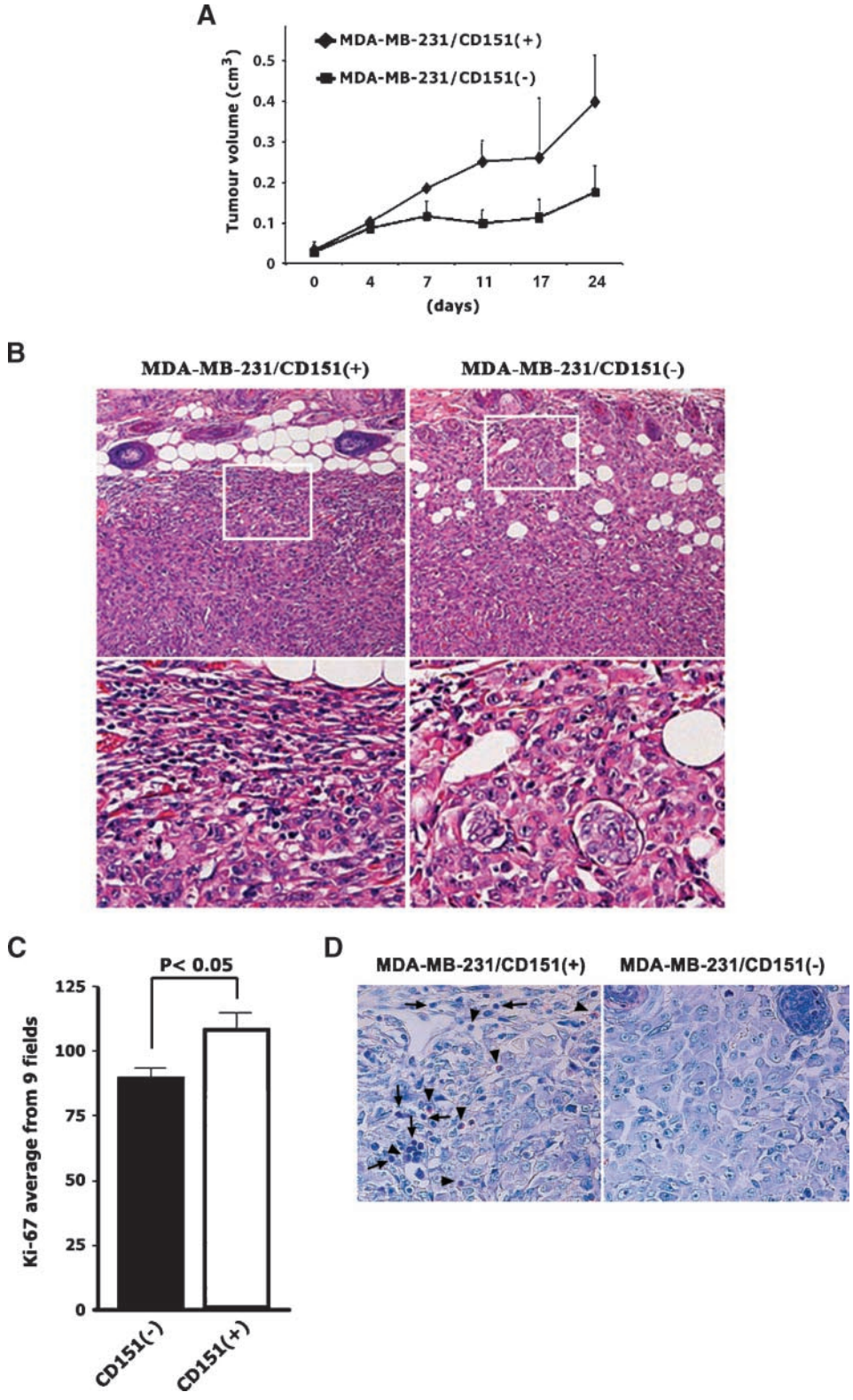

FIGURE 2. Down-regulation of CD151 causes inhibition of tumor cell growth. **A.** Tumor growth in mice. Growth of tumors was assessed after subcutaneous injection of MDA-MB-231/CD151(+) and MDA-MB-231/CD151(–) cells in athymic nude mice. Ten mice were used in each group. Tumors became measurable ~8 to 10 d posttransplantation; this is represented as day 0 on the graph. Points, means of tumor volumes evaluated at various time intervals; bars, SE. Presence of CD151 affects the histology of MDA-MB-231 xenografts. **B.** H&E staining of MDA-MB-231 xenografts. CD151(+) tumors are clearly separated from the epidermis by bands of loose tissue composed of interwoven strands of fibrin, endothelial and mesenchymal cells, and infiltrated by neutrophils (*left; inset;* magnification, ×200) whereas CD151 (–) tumor cells infiltrate the dermis with no apparent boundary between the nodule and the epidermis (*right; inset;* magnification, ×200). **C.** Ki-67 labeling index. Results of quantification of Ki-67–immunopositive cells (average from nine high-power fields, ~1,000 cells/sample; magnification, ×400). **D.** Giemsa staining of subcutaneous border MD-MB-231 xenografts. Differentiation of nuclear morphology of the cells reveals rich infiltration composed of lymphocytes (*arrows*) and granulocytes (*arrowheads*) in CD151(+) tumors (*left*) and almost absent from CD151(–) tumors (*right*).

length and thickness of the cables) were comparable in MDA-MB-231/CD151(+) and MDA-MB-231/CD151(−) cells. Similarly, we observed no difference in growth in the presence of fibroblasts when CD151-positive and CD151-depleted cells were seeded into three-dimensional Matrigel (Fig. 5B). We then examined whether coculturing with human endothelial cells affects the growth of CD151-positive and CD151-depleted MDA-MB-231 in three-dimensional Matrigel. In the presence

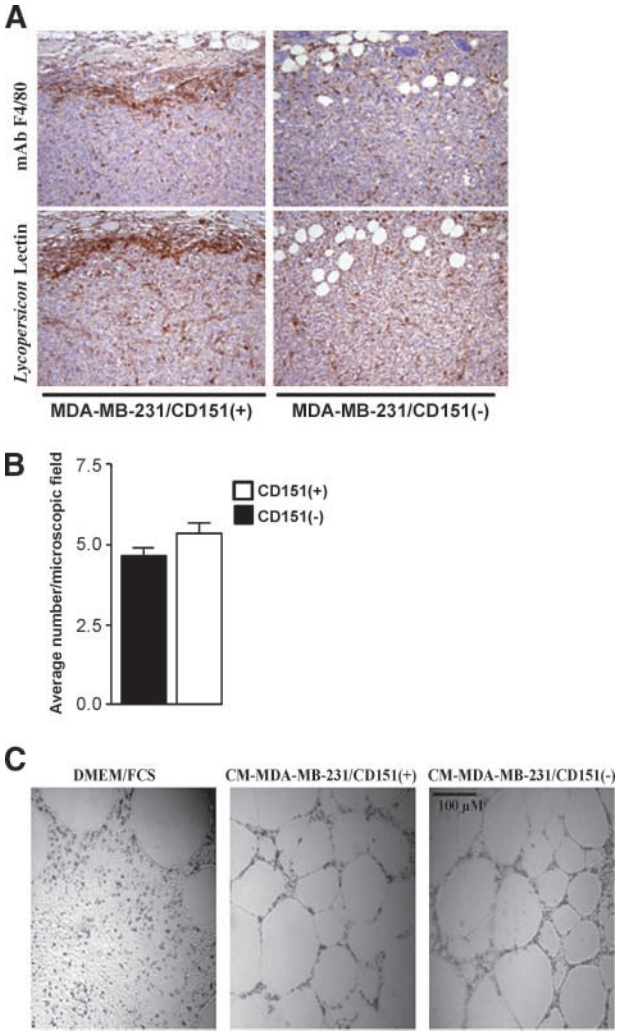

FIGURE 3. **A.** Subcutaneous zones of MDA-MB-231/CD151(+) (*left*) and MDA-MB-231/CD151(–) (*right*) xenografts (magnification, ×100). Immunohistochemistry: distribution of macrophages (*top*) and endothelial cells (*bottom*) was analyzed using monoclonal antibody F4/80 and biotinylated *L. esculentum* (tomato) lectin, respectively. Note the gradient of immunoreactivity which is particularly clearly prominent in CD151(+) xenografts. **B.** Vascularization of tumor xenografts. Analysis of vascularization was done as described in Materials and Methods. The numbers represent the average from nine counts per tumor. **C.** The effect of MDA-MB-231–conditioned medium (CM-MDA-MB-231) on endothelial cells (HUVEC). HUVEC were plated on polymerized Matrigel for 24 h in growth medium conditioned by MDA-MB-231/CD151(+) and MDA-MB-231/CD151(–) cells for 4 d.

of HUVEC, most of the MDA-MB-231/CD151(+) colonies (~65%) displayed a characteristic "scattering" phenotype (i.e., aggregates of loosely associated cells; Fig. 5C, *left*). By contrast, MDA-MB-231/CD151(−) cells were less responsive to HUVEC with >80% of the colonies retaining a "compact" morphology (Fig. 5C, *right*). In agreement with these findings, we observed specific differences in signaling when MDA-MB-231/CD151(+) and MDA-MB-231/CD151(−) cells were exposed to the medium conditioned by HUVEC. First, activation of extracellular signal-regulated kinase-1/2 (ERK1/2) was more robust in CD151-positive cells (Fig. 5D, *lanes 1-4*; Fig. 5E). Second, the dynamics of activation of Src kinases was also different. Whereas in MDA-MB-231/CD151(+) cells, the levels of active Src kinases have increased with prolonged incubations, the absence of CD151 reversed this trend (Fig. 5D, *lanes 1-4*). Importantly, the levels of active ERK1/2 and Src kinases were comparable when cells were plated on Matrigel in a standard growth medium (i.e., DMEM/10% fetal bovine serum; Fig. 5D, *lanes 5-8*). Furthermore, activation of PKB/c-Akt or basal levels of phosphorylation of FAK and p130Cas were not affected (Fig. 5D). To investigate whether such a selective effect of CD151 depletion on Src and Erk1/2 activation correlated with the behavior of MDA-MB-231 cells in three-dimensional Matrigel, we examined cellular growth in the presence of a specific Src (or MEK) inhibitor. In these experiments, we used

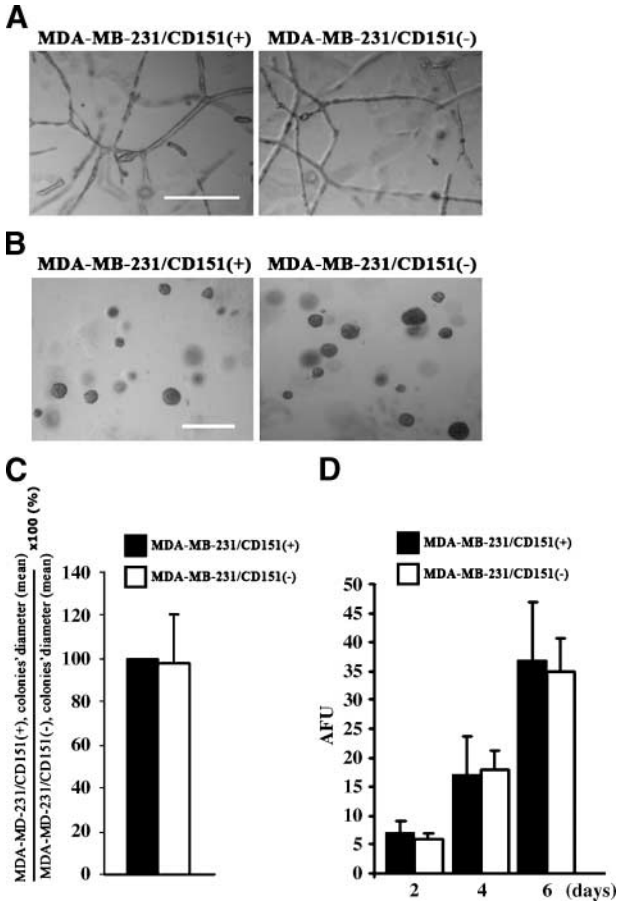

FIGURE 4. Contribution CD151 to growth in three-dimensional matrix. **A.** Growth in three-dimensional collagen. Cells were embedded into collagen gels as described in Materials and Methods and grown for 8 d. **B** to **D.** Growth in three-dimensional Matrigel. Cells were embedded into growth factor–reduced Matrigel as described in Materials and Methods and grown for 10 d. Bars, 200 μm. **C.** Quantification of colony sizes. Colony diameters were measured using ImageJ. The diameters of more than 50 colonies were measured for each of the cell lines in each of three separate experiments. Ratio of average colony diameter for CD151-positive and CD151-depleted MDA-MB-231 was calculated for each experiment. Columns, mean of ratios; bars, SD. **D.** Measurements of cell proliferation. Cell proliferation was measured using Alamar blue by a spectrofluorometric method. Columns, mean of two experiments (each in triplicate); bars, SD (*AFU,* arbitrary fluorescence units).

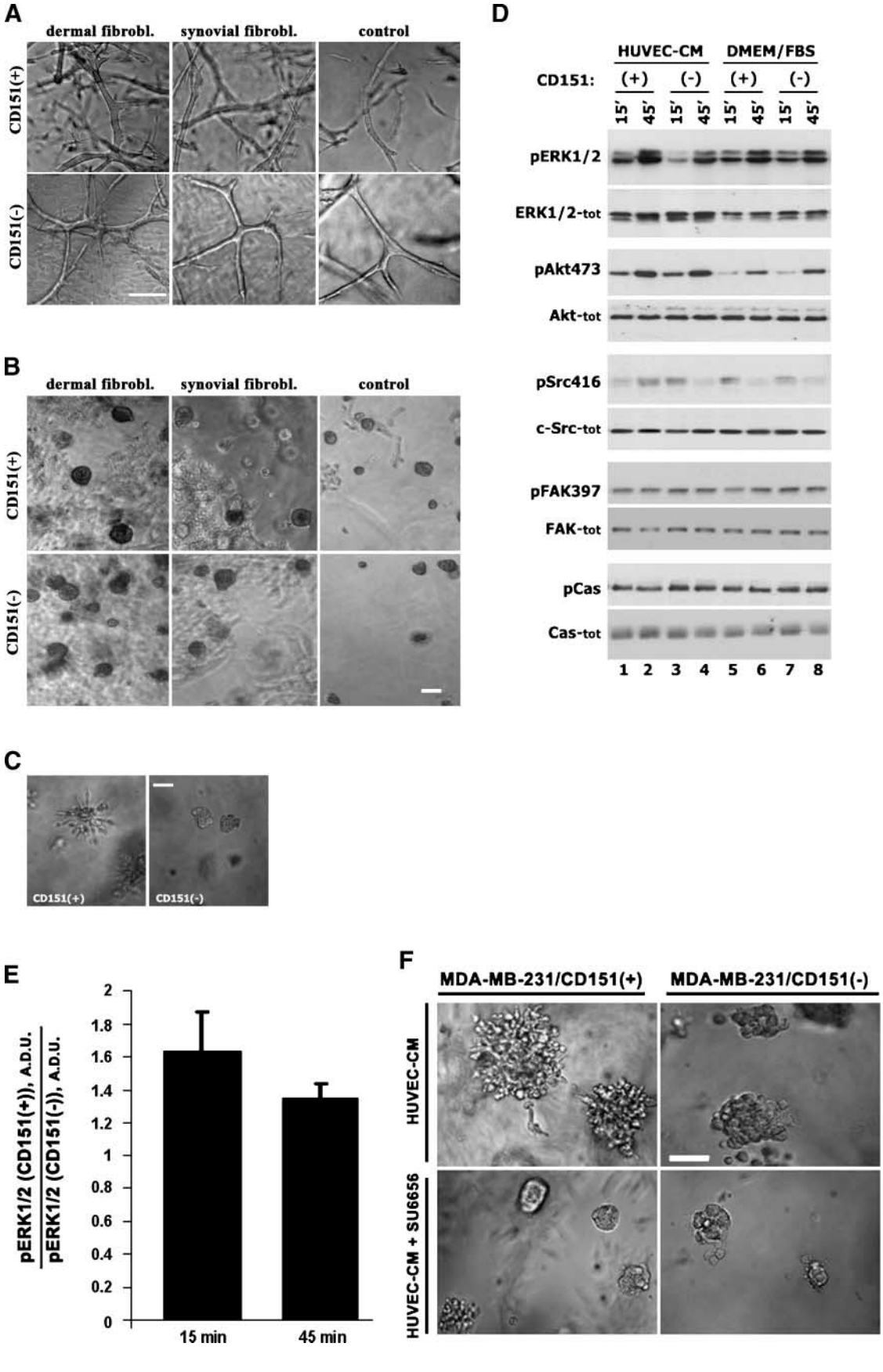
A
dermal fibrobl.
synovial fibrobl.
control
CD151(+)
CD151(-)
B
dermal fibrobl.
synovial fibrobl.
control
CD151(+)
CD151(-)
C
CD151(+)
CD151(-)
D
HUVEC-CM
DMEM/FBS
CD151:
(+)
(-)
(+)
(-)
15′
45′
15′
45′
15′
45′
15′
45′
pERK1/2
ERK1/2-tot
pAkt473
Akt-tot
pSrc416
c-Src-tot
pFAK397
FAK-tot
pCas
Cas-tot
1 2 3 4 5 6 7 8
E
pERK1/2 (CD151(+)), A.D.U.
pERK1/2 (CD151(-)), A.D.U.
2
1.8
1.6
1.4
1.2
1
0.8
0.6
0.4
0.2
0
15 min
45 min
F
MDA-MB-231/CD151(+)
MDA-MB-231/CD151(-)
HUVEC-CM
HUVEC-CM + SU6656

HUVEC-conditioned medium (HUVEC-CM) to avoid the potentially adverse effects of inhibitors on endothelial cells. Figure 5F illustrates that inhibition of Src kinases attenuated HUVEC-CM–induced growth and scattering of MDA-MB-231/CD151(+): the number of colonies which displayed a scattering phenotype decreased from ~72% to ~ 28%. On the other hand, despite the fact that in the presence of MEK1/2 inhibitor, UO126 growth of both CD151(+) and CD151(−) cells was impaired, no apparent effect on scattering of MDA-MB-231/CD151(+) in three-dimensional Matrigel was observed (results are not shown). These data strongly suggest that signaling via Src kinases contributes to CD151-dependent scattering induced by a HUVEC-produced soluble factor.

It has recently been reported that CD151 regulates cellular responses to EGF (24). Thus, we examined the behavior of MDA-MB-231/CD151(+) and MDA-MB-231/CD151(−) cells grown in three-dimensional ECM in the presence of EGF. As shown in Fig. 6A, the presence of EGF did not change the appearance or size of the colonies in three-dimensional Matrigel when compared with the control conditions. Furthermore, we observed no difference in EGF-induced or HB-EGF–induced tyrosine phosphorylation of cellular proteins, or activation of ERK1/2 and c-Akt (Fig. 6B). These results argue against the involvement of EGFR in the CD151-dependent cellular responses to an endothelial-derived soluble factor(s).

Association with Integrins Is Critical for CD151-Mediated Response of MDA-MB-231 Cells to HUVEC

To establish whether CD151-dependent sensitization to HUVEC involves integrins, we examined the responses of MDA-MB-231/CD151(−) cells which were engineered to express CD151-QRD mutant [MDA-MB-231/CD151(−)/rec/QRD cells]. A previous study has shown that mutation of QRD to INF (residues 194-196) within the large extracellular loop prevents direct interactions between CD151 and integrins within tetraspanin-enriched microdomains (31). We confirmed this observation using MDA-MB-231/CD151(−)/rec/QRD cells (25). As a control for these experiments, we used MDA-MB-231/CD151(−) cells re-expressing the wild-type CD151 [MDA-MB-231/CD151(−)/rec/wt cells]. Western blotting analysis showed that the expression levels of CD151-QRD mutant and wild-type protein in reconstituted cell lines were comparable (25). As expected, MDA-MB-231/CD151(−)/rec/wt cells regained their responsiveness to HUVEC (Fig. 7A, *left*) with >75% of the colonies exhibiting a scattering phenotype in three-dimensional Matrigel. On the contrary, the appearance of MDA-MB-231/CD151(−)/rec/QRD colonies was similar to that of the CD151-negative cells (Fig. 7A, *right*). In complementary experiments, we analyzed the contribution of integrins $\alpha3\beta1$ and $\alpha6\beta4$, principal integrin partners of CD151 in MDA-MB-231 cells, to HUVEC-induced cellular responses in three-dimensional ECM. Towards this end, we established stable MDA-MB-231 cell lines which expressed low levels of these integrins (referred to as MDA-MB-231/$\alpha3\beta1^{low}$ and MDA-MB-231/$\alpha6\beta4^{low}$). Flow cytometry experiments have shown that the levels of analyzed growth of $\alpha3\beta1$ and $\alpha6\beta4$ integrins were decreased by >90% (Fig. 7B). As illustrated in Fig. 7C, both MDA-MB-231/$\alpha3\beta1^{low}$ and MDA-MB-231/$\alpha6\beta4^{low}$ cells lost the ability to respond to the presence of endothelial cells and formed compact colonies in three-dimensional Matrigel. Taken together, these experiments show that the association with both $\alpha3\beta1$ and $\alpha6\beta4$ is critical for the CD151-dependent sensitization of tumor cells to soluble factors secreted by the endothelial cells.

Discussion

Our report identifies CD151 as an independent marker for poor prognosis in invasive ductal carcinoma of the breast and shows, for the first time, that increased expression of CD151 is associated with decreased overall survival. Furthermore, our xenograft experiments support the involvement of CD151 in breast cancer tumorigenesis and point to a new role for CD151 as a regulator of communication between tumor cells and the endothelium.

Previous work from this and other laboratories has shown that CD151 plays an important role in integrin-dependent invasive migration of tumor cells (32-34). Furthermore, using specific anti-CD151 monoclonal antibody, Zijlstra and colleagues found that CD151 may be involved in intravasation (15). However, this monoclonal antibody did not inhibit primary tumor growth. Here, we show that CD151 also plays a positive role in tumor cell growth *in vivo*. Interestingly, CD151 did not contribute to the inherent proliferative potential of tumor cells when they were grown in three-dimensional ECMs under standard culture conditions. These results suggest that increased proliferation of CD151-positive xenografts is dependent on host cells surrounding growing tumors. Indeed, we found that a deficiency in CD151 attenuated the responses of MDA-MB-231 to endothelial cells. We also showed that responses to a soluble factor(s) produced by endothelial cells require interactions between CD151 and integrins. This observation further strengthens the notion that tetraspanins are involved in the assembly of scaffolding platforms for lateral coordination of signaling pathways between various transmembrane receptors (4). As such, CD151 may link integrins with a receptor for the endothelium-derived soluble factor.

MDA-MB-231 cells express three principal CD151 integrin partners: $\alpha3\beta1$, $\alpha6\beta1$, and $\alpha6\beta4$. Although it remains to be established which of the CD151-integrin complexes contribute

FIGURE 5. Contribution of fibroblasts and endothelial cells to growth of MDA-MB-231 cells in three-dimensional ECM. Cells embedded in three-dimensional collagen (**A**) or Matrigel (**B** and **C**) were grown above the monolayer of fibroblasts (**A** and **B**) or HUVEC (**C**) as described in the legend to Fig. 4. Bars, 100 μm (**A**) or 50 μm (**B** and **C**). **D.** The effect of CD151 depletion on signaling. Serum-starved cells were detached using EDTA and subsequently resuspended in standard growth medium (DMEM/fetal bovine serum) or growth medium conditioned by HUVEC (HUVEC-CM). The cells were plated on Matrigel for the indicated time intervals and then scraped into Laemmli buffer. Proteins were resolved in 10% SDS-PAGE under reduced conditions. The proteins were transferred to a nitrocellulose membrane and probed with the indicated polyclonal antibodies. **E.** Densitometric analysis of activation Erk1/2 (i.e., measurements of pErk1/2) for the results in **D**. Measurements were done for two independent experiments (*A.D.U.*, arbitrary densitometry units). Note, the ratios of ~1.6 (for the 15-min time point) and ~1.3 (for the 45-min time point) indicate that the presence of CD151 potentiates HUVEC-CM–induced activation of Erk1/2. **F.** The effect of Src inhibitor on the growth of MDA-MB-231 cells in three-dimensional Matrigel. Cells were embedded in three-dimensional Matrigel and grown for 8 d in HUVEC-CM supplemented with 2 μmol/L of SU6656. The medium was changed every second day. Bar, 50 μm.

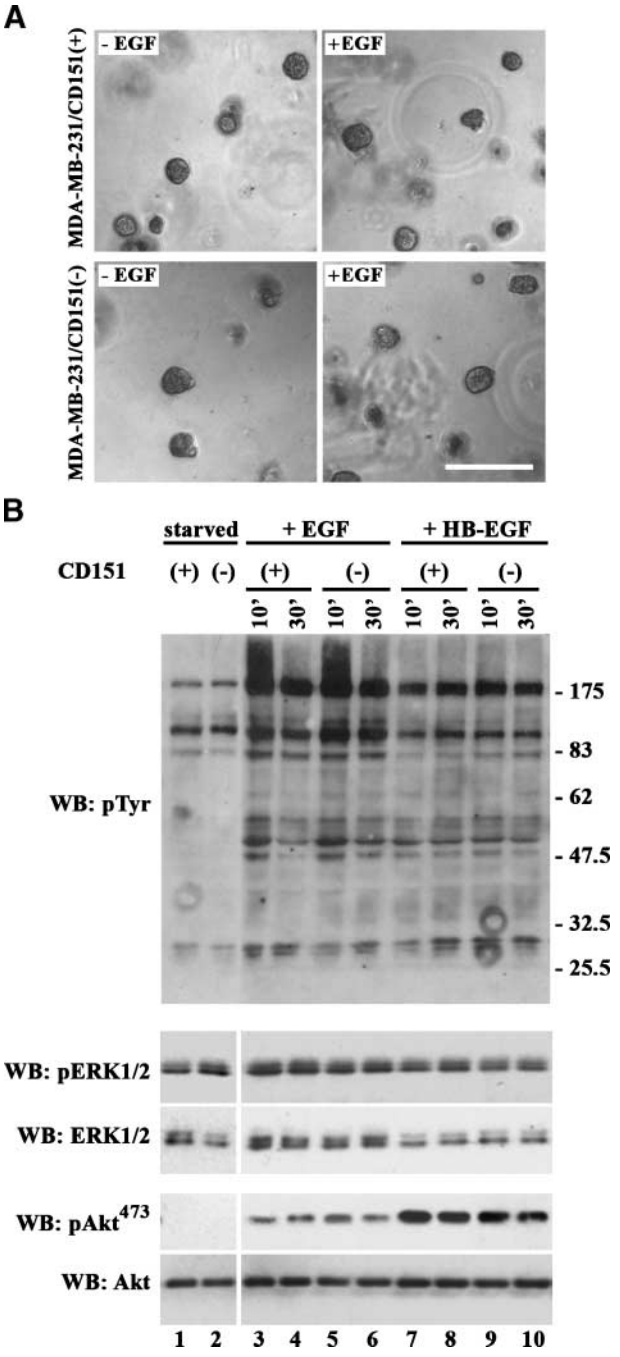

FIGURE 6. CD151-dependent cellular responses in three-dimensional Matrigel does not involve EGFR. **A.** Cells were embedded into growth factor–reduced Matrigel as described in Materials and Methods, and grown in the presence or absence of EGF (10 ng/mL) for 8 d. Bar, 200 μm. **B.** The effect of CD151 depletion on signaling via EGFR. Serum-starved cells were stimulated with EGF (50 ng/mL) or HB-EGF (50 ng/mL) for the indicated time intervals and then scraped into Laemmli buffer. Proteins were resolved in 10% SDS-PAGE under reduced conditions. The proteins were transferred to a nitrocellulose membrane and probed with the indicated polyclonal antibodies.

to the growth of MDA-MB-231 xenografts, it is likely that both α3β1-CD151 and α6β4-CD151 complexes are involved. Protumorigenic activity of α6β4 in breast cancer has been shown in various animal models (35-37), and this agrees with the observation that the elevated expression of this integrin is associated with significantly decreased overall survival of patients with breast cancer (38, 39). Similarly, the increased levels of α3β1 correlated with metastatic progression in breast cancer (40). Although further studies will be necessary to establish the clinical significance of this observation, we found that depletion of α3β1 integrin significantly inhibited both the growth of MDA-MB-231 cells in three-dimensional ECM *in vitro* and in xenograft experiments.[8]

It has been recently proposed that CD151 functions as a molecular linker between laminin-binding integrins (i.e., α3β1 and α6β1/4) and c-Met, a receptor for hepatocyte growth factor (HGF; ref. 23). The functional link between c-Met and integrins is also supported by the observation that HGF can

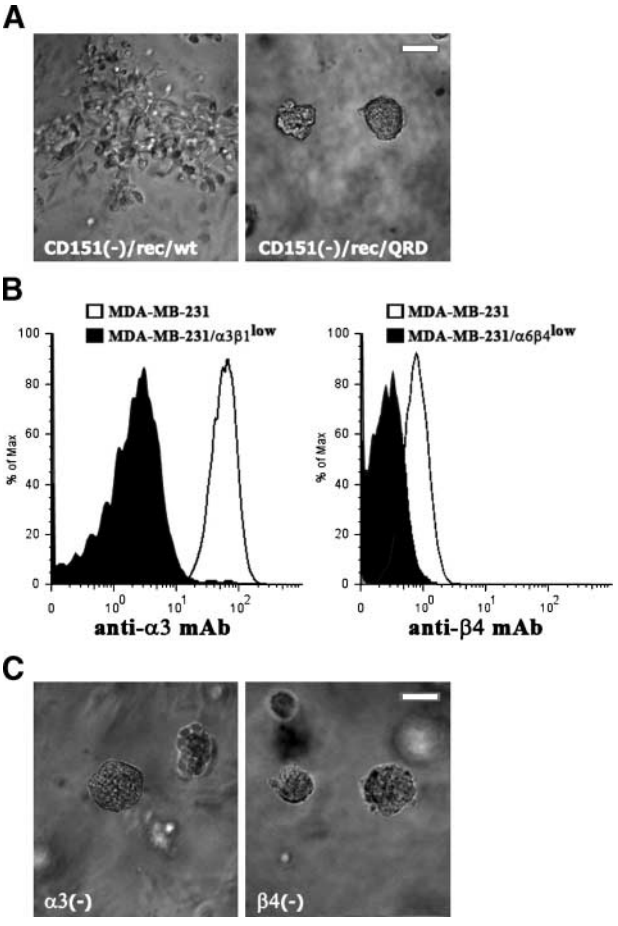

FIGURE 7. The role of integrins in CD151-dependent cellular responses to endothelial cells. **A** and **C.** Various derivatives of MDA-MB-231 cells were plated in three-dimensional Matrigel and grown in the presence of HUVEC as described in Fig. 5. Bars, 50 μm. **B.** Generation of stable α3β1-depleted and α6β4-depleted cells. Down-regulation of integrins in MDA-MB-231 cells was analyzed by flow cytometry. Cells stained with mouse monoclonal antibody against either α3 (A3-IVA5; *left histogram*) or β4 (3E1; *right histogram*) integrin subunits.

[8] R. Sadej, K. Gkirtzimanaki, A.G. Eliopoulos, F. Berditchevski, unpublished results.

stimulate integrin avidity (41). However, it is unlikely that CD151-dependent differential responses to HUVEC are caused by deficiencies in the HGF → c-Met signaling axis in MDA-MB-231/CD151(−) cells. First, HUVEC do not seem to produce HGF (42). Second, the absence of CD151 did not affect the growth pattern of breast cancer cells in three-dimensional ECM in coculture experiments with dermal fibroblasts, a rich source of HGF (43). Recently, Yang and colleagues suggested that the protumorigenic function of CD151 may involve signaling via EGFR (24). Our results clearly indicate that the growth of MDA-MB-231/CD151(+) and MDA-MB-231/CD151(−) cells in three-dimensional ECM is not affected by the presence of EGF. Furthermore, we have thus far been unable to identify the difference(s) between CD151-positive and CD151-negative MDA-MB-231 cells when we analyzed various signaling pathways triggered by EGF. In a recent study, we showed that invasiveness through Matrigel along the gradient of EGF is controlled by the CD151-α3β1 complex (25). These results, and the observation by Yang and colleagues, agree with the concept that CD151 may be involved in the coordination of signals via laminin-binding integrins and EGFR, and this is likely to play an important role in tumor cell invasiveness and metastasis. However, the results presented here argue against the involvement of an EGFR-CD151-integrin signaling axis in the growth of MDA-MB-231 cells in the animal model. Identification of the relevant ligand-receptor pair and dissection of signaling pathways leading to the activation of ERK1/2 and Src kinases should clarify the role played by CD151 in the transmission of the signal from endothelial cells and shed light on the involvement of CD151 in tumor cell growth *in vivo*.

Distinct patterns of vascularization observed in CD151-positive and CD151-negative xenografts may explain the subtle differences in histologic appearance of the tumors and distribution of tumor-infiltrating macrophages. Furthermore, a more pronounced effect on proliferation at the deep border of the tumor (judged by the Ki-67 index) may suggest a less efficient supply of endothelium-derived or macrophage-derived growth factors to CD151(−) tumors. Conversely, the diminished growth rate of CD151-negative cells may have a lower metabolic demand, and consequently, induces less pronounced vascularization of xenografts. Of interest, the protumorigenic function of another tetraspanin (CO-029/Tspan8/D6.1A) in pancreatic tumor cells was also associated with the paracrine activity of the protein (12, 44). Induction of angiogenesis by the Tspan8-expressing tumors seems to involve tumor-derived exosomes and, in part, increased the production of VEGF and matrix metalloproteinase-13 (12). Although culture medium conditioned by MDA-MB-231 can also affect *in vitro* angiogenesis (45), we found that the absence of CD151 did not influence the modulatory activity of the medium conditioned by these cells. Although more studies are necessary to dissect a complex circuitry of communication between tumor cells and vasculature, our data indicate that CD151-dependent paracrine activity of MDA-MB-231 is likely to require contributions from other components of the tumor microenvironment (e.g., macrophages).

We have shown that elevated expression of CD151 inversely correlates with overall survival of breast cancer patients with invasive ductal carcinoma. More detailed analysis is necessary to establish whether overexpression of CD151 is associated with any of the five distinct subtypes of breast cancer (46). In this regard, we did not observe a significant correlation between the overexpression of CD151 and ER and progesterone receptor status in our invasive ductal breast adenocarcinoma samples. These results are at odds with the report by Yang and colleagues, who observed elevated expression of CD151 in 45% of ER-negative breast tumors. Although more work is required to draw a definitive conclusion, we would like to emphasize that in contrast to the work by Yang and colleagues, our analysis was done on a homogenous group of specimens (i.e., invasive ductal carcinomas).

In summary, we have shown that tetraspanin CD151 regulates the growth of breast cancer cells *in vivo* by controlling their communication with endothelial cells. Importantly, our data link the overexpression of CD151 with lower survival of patients with breast cancer, thereby identifying this tetraspanin as an independent prognostic marker and potential novel target for developing new therapies.

Materials and Methods

Cells, Antibodies, and Reagents

MDA-MB-231 cells were grown in DMEM (Sigma) supplemented with 10% fetal bovine serum. Fibroblasts were derived from either the synovium or skin of patients with arthritis undergoing joint replacement, and then isolated and cultured as described (47). HUVEC (PromoCell) were grown in endothelial cell growth medium with SupplementMix (PromoCell). The mouse anti-CD151 monoclonal antibodies were 5C11 (48), 11B1G4 (provided by Dr. L. Ashman, University of Newcastle, Australia), and NCL-CD151 (Novocastra). Rabbit polyclonal anti-human Ki-67 antibody was from Abcam, rat anti-mouse F4/80 antigen monoclonal antibody was from AbD Serotec, rabbit anti-human FGF2 antibody was from Santa Cruz Biotechnology, and mouse anti-human VEGF monoclonal antibody was from BD PharMingen. Anti-phosphorylated FAK (Tyr^{397}) antibody was purchased from BD Bioscience, and anti–β-actin was from Sigma. The rest of the antibodies used in this study were purchased from Cell Signaling Technology. Biotinylated *L. esculentum* lectin (Vector Labs) was used to identify mouse endothelial cells.

Construction of MDA-MB-231 Knockdown Cell Lines

Generation of MDA-MB-231/CD151(+), MDA-MB-231/CD151(−), MDA-MB-231/CD151rec, and MDA-MB-231/CD151-QRD stable cell lines were described earlier (25). MDA-MB-231/$\alpha3\beta1^{low}$ cells were established from MDA-MB-231/CD151(+) by fluorescent sorting of the cells expressing short-hairpin RNA (shRNA) that specifically targets the α3 integrin subunit (target sequence is 5′-gctacatgattcagcgcaa-3′). MDA-MB-231/$\alpha6\beta4^{low}$ cells were generated using a specific shRNA construct which targets the β4 integrin subunit (35).

Assessment of Cell Growth in Three-dimensional ECM

Growth in Matrigel. Three drops of cell suspension in Matrigel (~1.5×10^3/40 μL) were plated onto a tissue culture plate and incubated at 37°C for up to 30 min to solidify. Solidified Matrigel drops were covered with growth medium. Colonies

were photographed 10 d after plating. Relative size of the colonies was determined by measuring 60 to 100 random colonies in each drop using ImageJ software. At least two independent experiments were carried out for each cell line.

Growth in collagen. Cells were suspended in 1.6 mg/mL of rat tail collagen type I (~1.5×10^3/40 μL) and grown for 7 to 8 d. Colonies were analyzed using Zeiss Axiovert 25 microscope. In coculture experiments, fibroblasts (or HUVEC) were grown in 48-well plates until they reached ~80% confluence. Subsequently, MDA-MB-231 cells (~8×10^3/200 μL) suspended in collagen or Matrigel were overlaid and the cultures continued to grow for an additional 7 to 10 d with growth medium being replaced every 48 h.

Western Blotting

Growing cells were scraped and lysed in the presence of ice-cold Laemmli buffer/protease inhibitor cocktail. An equal amount of protein from each sample was loaded per lane, separated by SDS-PAGE, and transferred onto a nitrocellulose membrane. Proteins were probed with specific antibodies in PBS/0.2% Tween 20, or TBST in case of further detection of phosphoproteins. Secondary antibodies conjugated to horseradish peroxidase and Western Lighting Chemiluminescence Reagent Plus (Perkin-Elmer) were used to develop images.

Analysis of Activation of FAK, Src, PKB/cAkt, ERK1/2, and Phosphorylation of p130Cas

The serum-starved cells (12-16 h in DMEM) were detached with 2 mmol/L of EDTA, and subsequently resuspended in DMEM/10% fetal bovine serum, or endothelial medium conditioned by HUVEC for 2 d. Cell suspension was plated onto dishes preabsorbed with Matrigel (20 μg/mL) for different lengths of time. The cells were scraped into Laemmli sample buffer supplemented with 2 mmol/L of phenylmethylsulfonyl fluoride, 10 μg/mL of aprotinin, 10 μg/mL of leupeptin, 100 μmol/L of Na_3VO_4, 10 mmol/L of NaF, and 10 mmol/L of $Na_3P_4O_7$. Cellular proteins were resolved in 10% SDS-PAGE, transferred to the nitrocellulose membrane, and probed with the appropriate phosphospecific antibody.

Xenograft Experiments

Female athymic nude Foxn1 *nu*/*nu* mice at 6 wk of age were purchased from Harlan, Italy. Mice were injected subcutaneously (above the hind leg) with 5×10^6 cells resuspended in 150 μL of HBSS (Invitrogen) per mouse. Six to 10 animals per group were used in the experiments. Tumor growth was monitored every other day and tumor volume was measured with a Caliper instrument. Tumor volume (V) was calculated by the "ellipsoid" formula: $V = a \times b \times [(a + b) / 2] \times \pi/6$, where a represents the minimum and b the maximum tumor diameter. Tumors were fixed in 10% buffered formalin and processed for histologic and immunohistochemical analyses. All experiments were done in accordance with institutional and national animal research guidelines.

Immunohistochemistry

Antibodies to (*a*) CD151 (mouse anti-human, dilution 1:50), (*b*) Ki-67 (rabbit anti-human, dilution 1:25), (*c*) F4/80 antigen (rat anti-mouse, dilution 1:180), (*d*) FGF2 (rabbit anti-human, dilution 1:50), (*e*) VEGF (mouse anti-human, dilution 1:200), and (*f*) biotinylated *L. esculentum* lectin (dilution 1:50) were used. After antigen retrieval, immunostaining of paraffin sections was done using a standard avidin-biotin-peroxidase complex method. The sections counterstained with hematoxylin were analyzed and images captured using the Olympus DP70 camera and the Olympus DP-Soft software (Japan). Tumor vascularization was assessed using the Chalkley method (49). The "hotspots" were at low (40×) magnification in three distinct areas: (*a*) superficial (subcutaneous); (*b*) central (adjacent to necrotic areas), and (*c*) close to the deep margin of the tumor. The number of vessels (no. [CD151(−)] = 9; no. [CD151(+)] = 9) was counted in nine high-power (400×) fields corresponding to 0.0625 mm^2 from regions a to c. The numbers represent the average from nine counts.

Proliferative Index in Tumor Sections

For each tissue sample, immunostaining with antibody to Ki-67 was assessed by two independent observers. Only nuclear immunoreactivity was considered positive. Initially, the entire section was assessed at low magnification (40×) and three distinct regions of cell proliferation were identified: (*a*) superficial (subcutaneous), (*b*) central (adjacent to necrotic areas), and (*c*) close to the deep margin of the tumor. The number of Ki-67–immunopositive cells in each sample (no. [CD151(−)] = 9; no. [CD151(+) = 9]) was counted in nine high-power (400×) fields from proliferation regions a to c (~1,000 cells/section). The mean ± SE were calculated and statistical analyses were carried out by the unpaired t test using a GraphPad Prism 3.2 program (GraphPad Software).

Analysis of CD151 Immunohistochemical Expression in Clinical Samples

Fifty-six specimens of primary invasive ductal carcinoma (patients treated between 1998 and 2001) were obtained from the archives of the Department of Oncology of Copernicus Memorial Hospital (Lodz, Poland) following the local ethics regulations. The disease was staged according to the tumor-node-metastasis system and samples histologically graded using the Nottingham Criteria. Pathologic analysis and surgical evaluation confirmed the tissue diagnosis and the clinical stage of disease. Follow-up period was defined as the time from surgery to the last observation for censored cases or death for complete observations. Five-micrometer formalin-fixed, paraffin-embedded sections were processed for routine histology and immunohistochemistry for ER (dilution 1:35; Dako, PL) and CD151 (dilution 1:50; Novocastra). Immunostaining was done after antigen retrieval by microwaving the sections for 8 min in citrate buffer (pH 6.0) and using the EnVision kit (Dako, PL) according to the protocols of the manufacturer. Assessment of CD151 immunoreactivity was as follows: (*a*) negative—no staining or uniform membrane positivity in <10% of the tumor cells; (*b*) positive—a weak to strong complete membrane staining observed in >10% of the tumor cells. Scoring for ER nuclear expression was done using the method described by McCarty et al. (50). Tumors were considered positive for ER with a Histo-score of ≥100.

Statistical analysis. Overall survival was calculated from the date of surgery to the date of death, or the last follow-up, as recommended by the Kaplan-Meier method. Differences in

survival distributions were compared using log rank test. Data for patients who died from causes other than breast cancer were censored at the time of death. Univariate analyses of overall survival were done using the Cox proportional hazards regression model. Pearson's χ^2 test was used to assess the associations between CD151 expression and clinicopathologic variables. The results were considered statistically significant when two-sided P values were <0.050. The analyses were done using the StatsDirect software (StatsDirect, Ltd.).

Disclosure of Potential Conflicts of Interest

No potential conflicts of interest were disclosed.

Acknowledgments

We are very grateful to all our colleagues for their generous gifts of the reagents that were used in this study.

References

1. Hemler ME. Tetraspanin proteins mediate cellular penetration, invasion, and fusion events and define a novel type of membrane microdomain. Annu Rev Cell Dev Biol 2003;19:397–422.

2. Hemler ME. Tetraspanin functions and associated microdomains. Nat Rev Mol Cell Biol 2005;6:801–11.

3. Yunta M, Lazo PA. Tetraspanin proteins as organisers of membrane microdomains and signalling complexes. Cell Signal 2003;15:559–64.

4. Levy S, Shoham T. The tetraspanin web modulates immune-signalling complexes. Nat Rev Immunol 2005;5:136–48.

5. Dong J-T, Lamb PW, Rinker-Schaeffer CW, et al. KAI 1, a metastasis suppressor gene for prostate cancer on human chromosome 11p11.2. Science 1995;268: 884–6.

6. Takaoka A, Hinoda Y, Sato S, et al. Reduced invasive and metastatic potentials of KAI1-transfected melanoma cells. Jpn J Cancer Res 1998;89:397–404.

7. Yang X, Wei LL, Tang C, et al. Overexpression of KAI1 suppresses *in vitro* invasiveness and *in vivo* metastasis in breast cancer cells. Cancer Res 2001;61: 5284–8.

8. Ovalle S, Gutierrez-Lopez MD, Olmo N, et al. The tetraspanin CD9 inhibits the proliferation and tumorigenicity of human colon carcinoma cells. Int J Cancer 2007;121:2140–52.

9. Ikeyama S, Koyama M, Yamaoko M, et al. Suppression of cell motility and metastasis by transfection with human motility-related protein (MRP-1/CD9) DNA. J Exp Med 1993;177:1231–7.

10. He B, Liu L, Cook GA, et al. Tetraspanin CD82 attenuates cellular morphogenesis through down-regulating integrin α6-mediated cell adhesion. J Biol Chem 2005;280:3346–54.

11. Odintsova E, Sugiura T, Berditchevski F. Attenuation of EGF receptor signaling by a metastasis suppressor tetraspanin KAI-1/CD82. Curr Biol 2000;10: 1009–12.

12. Gesierich S, Berezovskiy I, Ryschich E, et al. Systemic induction of the angiogenesis switch by the tetraspanin D6.1A/CO-029. Cancer Res 2006;66: 7083–94.

13. Tokuhara T, Hasegawa H, Hattori N, et al. Clinical significance of CD151 gene expression in non-small cell lung cancer. Clin Cancer Res 2001;7: 4109–14.

14. Ang J, Lijovic M, Ashman LK, et al. CD151 protein expression predicts the clinical outcome of low-grade primary prostate cancer better than histologic grading: a new prognostic indicator? Cancer Epidemiol Biomarkers Prev 2004;13: 1717–21.

15. Zijlstra A, Lewis J, Degryse B, et al. The inhibition of tumor cell intravasation and subsequent metastasis via regulation of *in vivo* tumor cell motility by the tetraspanin CD151. Cancer Cell 2008;13:221–34.

16. Kohno M, Hasegawa H, Miyake M, et al. CD151 enhances cell motility and metastasis of cancer cells in the presence of focal adhesion kinase. Int J Cancer 2002;97:336–43.

17. Chometon G, Zhang ZG, Rubinstein E, et al. Dissociation of the complex between CD151 and laminin-binding integrins permits migration of epithelial cells. Exp Cell Res 2006;312:983–95.

18. Garcia-Lopez MA, Barreiro O, Garcia-Diez A, et al. Role of tetraspanins CD9 and CD151 in primary melanocyte motility. J Invest Dermatol 2005;125: 1001–9.

19. Shigeta M, Sanzen N, Ozawa M, et al. CD151 regulates epithelial cell-cell adhesion through PKC- and Cdc42-dependent actin cytoskeletal reorganization. J Cell Biol 2003;163:165–76.

20. Takeda Y, Kazarov AR, Butterfield CE, et al. Deletion of tetraspanin Cd151 results in decreased pathologic angiogenesis *in vivo* and *in vitro*. Blood 2007;109: 1524–32.

21. Yanez-Mo M, Alfranca A, Cabañas C, et al. Regulation of endothelial cell motility by complexes of tetraspan molecules CD81/TAPA-1 and CD151/PETA-3 with α3β1 integrin localized at endothelial lateral junctions. J Cell Biol 1998;141: 791–804.

22. Winterwood NE, Varzavand A, Meland MN, et al. A critical role for tetraspanin CD151 in α3β1 and α6β4 integrin-dependent tumor cell functions on laminin-5. Mol Biol Cell 2006;17:2707–21.

23. Klosek SK, Nakashiro K, Hara S, et al. CD151 forms a functional complex with c-Met in human salivary gland cancer cells. Biochem Biophys Res Commun 2005;336:408–16.

24. Yang XH, Richardson AL, Torres-Arzayus MI, et al. CD151 accelerates breast cancer by regulating α6 integrin function, signaling, and molecular organization. Cancer Res 2008;68:3204–13.

25. Baldwin G, Novitskaya V, Sadej R, et al. Tetraspanin cd151 regulates glycosylation of α3β1 integrin. J Biol Chem 2008;283:35445–54.

26. Gerdes J, Becker MH, Key G, et al. Immunohistological detection of tumour growth fraction (Ki-67 antigen) in formalin-fixed and routinely processed tissues. J Pathol 1992;168:85–6.

27. Austyn JM, Gordon S. F4/80, a monoclonal antibody directed specifically against the mouse macrophage. Eur J Immunol 1981;11:805–15.

28. Mazzetti S, Frigerio S, Gelati M, et al. *Lycopersicon esculentum* lectin: an effective and versatile endothelial marker of normal and tumoral blood vessels in the central nervous system. Eur J Histochem 2004;48:423–8.

29. Luqmani YA, Graham M, Coombes RC. Expression of basic fibroblast growth factor, FGFR1 and FGFR2 in normal and malignant human breast, and comparison with other normal tissues. Br J Cancer 1992;66:273–80.

30. Zhang W, Ran S, Sambade M, et al. A monoclonal antibody that blocks VEGF binding to VEGFR2 (KDR/Flk-1) inhibits vascular expression of Flk-1 and tumor growth in an orthotopic human breast cancer model. Angiogenesis 2002;5:35–44.

31. Kazarov AR, Yang X, Stipp CS, et al. An extracellular site on tetraspanin CD151 determines α3 and α6 integrin-dependent cellular morphology. J Cell Biol 2002;158:1299–309.

32. Sugiura T, Berditchevski F. Function of a3b1-tetraspanin protein complexes in tumor cell invasion. Evidence for the role of the complexes in production of matrix metalloproteinase 2 (MMP-2). J Cell Biol 1999;146: 1375–89.

33. Hong IK, Jin YJ, Byun HJ, et al. Homophilic interactions of the tetraspanin CD151 up-regulate motility and MMP-9 expression of human melanoma cells through adhesion-dependent c-jun activation signaling pathways. J Biol Chem 2006;281:24279–92.

34. Shiomi T, Inoki I, Kataoka F, et al. Pericellular activation of proMMP-7 (promatrilysin-1) through interaction with CD151. Lab Invest 2005;85: 1489–506.

35. Lipscomb EA, Simpson KJ, Lyle SR, et al. The α6β4 integrin maintains the survival of human breast carcinoma cells *in vivo*. Cancer Res 2005;65: 10970–6.

36. Bon G, Folgiero V, Bossi G, et al. Loss of β4 integrin subunit reduces the tumorigenicity of MCF7 mammary cells and causes apoptosis upon hormone deprivation. Clin Cancer Res 2006;12:3280–7.

37. Guo W, Pylayeva Y, Pepe A, et al. β4 integrin amplifies ErbB2 signaling to promote mammary tumorigenesis. Cell 2006;126:489–502.

38. Diaz LK, Cristofanilli M, Zhou X, et al. β4 integrin subunit gene expression correlates with tumor size and nuclear grade in early breast cancer. Mod Pathol 2005;18:1165–75.

39. Lu S, Simin K, Khan A, et al. Analysis of integrin β4 expression in human breast cancer: association with basal-like tumors and prognostic significance. Clin Cancer Res 2008;14:1050–8.

40. Morini M, Mottolese M, Ferrari N, et al. The α3β1 integrin is associated with mammary carcinoma cell metastasis, invasion, and gelatinase B (MMP-9) activity. Int J Cancer 2000;87:336–42.

41. Trusolino L, Cavassa S, Angelini P, et al. HGF/scatter factor selectively promotes cell invasion by increasing integrin avidity. FASEB J 2000;14: 1629–40.

42. Kobayashi H, DeBusk LM, Babichev YO, et al. Hepatocyte growth factor mediates angiopoietin-induced smooth muscle cell recruitment. Blood 2006;108: 1260–6.

43. Takami Y, Yamamoto I, Tsubouchi H, et al. Modulation of hepatocyte growth factor induction in human skin fibroblasts by retinoic acid. Biochim Biophys Acta 2005;1743:49–56.

44. Claas C, Seiter S, Claas A, et al. Association between the rat homologue of CO-029, a metastasis-associated tetraspanin molecule and consumption coagulopathy. J Cell Biol 1998;141:267–80.

45. Bajou K, Lewalle JM, Martinez CR, et al. Human breast adenocarcinoma cell lines promote angiogenesis by providing cells with uPA-PAI-1 and by enhancing their expression. Int J Cancer 2002;100:501–6.

46. Sorlie T. Molecular portraits of breast cancer: tumour subtypes as distinct disease entities. Eur J Cancer 2004;40:2667–75.

47. Filer A, Parsonage G, Smith E, et al. Differential survival of leukocyte subsets mediated by synovial, bone marrow, and skin fibroblasts: site-specific versus activation-dependent survival of T cells and neutrophils. Arthritis Rheum 2006; 54:2096–108.

48. Berditchevski F, Chang S, Bodorova J, Hemler ME. Generation of Monoclonal Antibodies to Integrin-associated Proteins. Evidence that $\alpha 3$ $\beta 1$ complexes with emmprin/basigin/OX47/M6. J Biol Chem 1997;272:29174–80.

49. Fox SB, Leek RD, Smith K, Hollyer J, Greenall M, Harris AL. Tumor angiogenesis in node-negative breast carcinomas-relationship with epidermal growth factor receptor, estrogen receptor, and survival. Breast Cancer Res Treat 1994;29:109–16.

50. McCarty KS, Jr., Miller LS, Cox EB, et al. Estrogen receptor analyses. Correlation of biochemical and immunohistochemical methods using monoclonal antireceptor antibodies. Arch Pathol Lab Med 1985;109:716–21.